

A New Family of Variational-Form-Based Regularizers for Reconstructing Epicardial Potentials from Body-Surface Mapping

DF Wang, RM Kirby, RS MacLeod, CR Johnson

Scientific Computing and Imaging Institute, University of Utah, Salt Lake City, UT, USA

Abstract

We propose a new family of regularizers for the inverse ECG problem, using a variational principle that underlies finite element approximation methods. As an alternative to traditional Tikhonov regularizers, the variational formulation has several advantages: 1)it enables a simple construction of the gradient operator (in a matrix form) over irregular meshes, which is often difficult to derive; 2)it achieves consistent regularization under multi-scale simulations by preserving the norm, which is evaluated by the resolution-independent L_2 -norm rather than the discrete Euclidean norm; and 3)it allows simultaneous application of multiple constraints efficiently. Our proposed method is validated by simulation on a realistic 3D model with clinical heart data, showing that the variational formulation may improve a broader range of potential-based electrocardiographic problems.

1. Introduction

This paper studies one type of inverse problem in electrocardiography (ECG): non-invasively recovering epicardial potentials from body-surface recordings. The underlying bioelectric model is a potential-based boundary value problem with the Laplace’s equation. Using finite elements or boundary elements, the equation is numerically solved over the source-free volume between the heart and torso surfaces, yielding a transfer matrix \mathbf{K} that relates the epicardial potentials \mathbf{u}_H with the torso potentials \mathbf{u}_T : $\mathbf{K}\mathbf{u}_H = \mathbf{u}_T$. The inverse calculation involves solving \mathbf{u}_H given \mathbf{K} and \mathbf{u}_T .

The matrix \mathbf{K} is well-known to be severely ill-conditioned due to the ill-posed nature of the inverse problem. One common method for stabilizing the inverse solution is the Tikhonov regularization:

$$\mathbf{u}_H = \operatorname{argmin} \{ \|\mathbf{K}\mathbf{u}_H - \mathbf{u}_T\|_2^2 + \lambda^2 (\|\mathbf{L}\mathbf{u}_H\|_2^2) \} \quad (1)$$

where $\|\cdot\|_2$ is the Euclidean norm. The first term is the residual error whereas the second term is a regularizer constraining certain property of the epicardial potentials. There are three basic Tikhonov schemes based on

the choice for \mathbf{L} . The zero-order Tikhonov (ZOT) takes \mathbf{L} as an identity matrix, constraining the amplitude of epicardial potentials. The first-order Tikhonov (FOT) takes \mathbf{L} as a gradient operator, constraining the spatial derivative of potentials. The second-order Tikhonov (SOT) takes \mathbf{L} as a surface Laplacian operator and constrains the curvature.

While there are several ad-hoc local approximation techniques in the literature, few explain how to derive the gradient operator in an explicit matrix form over irregular meshes. The matrix form is needed for implementing FOT or the total-variation regularization, but given an irregular mesh it is hard to determine weights over neighboring nodes. We formulate a gradient operator by adopting the variational principles underlying the finite element method. We then generalize the variational formulation and propose a family of new regularizers for ZOT, SOT or other Sobolev-norm regularizations. These “variational-formed” regularizers convey similar ideas to traditional regularizers, but have advantages such as numerical efficiency, allowing imposition of multiple constraints, and consistent regularization under multi-scale simulation.

2. Method

Variational-Formed Gradient Operator. We rewrite the Tikhonov regularization (1) using the continuous L_2 -norm:

$$\|\mathbf{K}\tilde{\mathbf{u}}_H - \tilde{\mathbf{u}}_T\|_{L_2}^2 + \lambda^2 \|\mathbf{L}\tilde{\mathbf{u}}_H\|_{L_2}^2 \quad (2)$$

where $\tilde{\mathbf{u}}_H$ and $\tilde{\mathbf{u}}_T$ denote continuous potential fields. $\|\cdot\|_{L_2}$ the norm of a continuous function, given by:

$$\|u\|_{L_2}^2 = (u, u) = \int_H u \cdot u d\Omega \quad (3)$$

Let $\{\phi_i(\mathbf{x})\}$ denote the finite element basis function associated with node i on the heart surface mesh \mathcal{H} , and \mathbf{u}_H be the vector of potentials on mesh nodes. By finite element formulation, $\tilde{\mathbf{u}}_H = \sum_k \mathbf{u}_H^k \phi_k$, $k \in \mathcal{H}$. The L_2 -norm of the potential gradient field on \mathcal{H} can be written as

$$\|\nabla \tilde{\mathbf{u}}_H\|_{L_2}^2 = \left(\sum_i \mathbf{u}_H^i \nabla \phi_i, \sum_j \mathbf{u}_H^j \nabla \phi_j \right) = \mathbf{u}_H^T \mathbf{S} \mathbf{u}_H \quad (4)$$

where \mathbf{S} is the stiffness matrix defined over the heart surface. For the first-order Tikhonov, \mathbf{L} in (2) can be taken as the Cholesky factor of \mathbf{S} : $\mathbf{L}^T \mathbf{L} = \mathbf{S}$. Such an \mathbf{L} can be viewed as a variational form of the gradient operator. To justify this formulation, recall that if \mathbf{L} is the discrete gradient operator such that $\mathbf{L}\mathbf{u} = \nabla\mathbf{u}$, it should satisfy $\|\nabla\mathbf{u}_H\|^2 = \|\mathbf{L}\mathbf{u}_H\|_2^2 = \mathbf{u}_H^T \mathbf{L}^T \mathbf{L} \mathbf{u}_H$. Equating this expression with (4) gives $\mathbf{L}^T \mathbf{L} = \mathbf{S}$.

Generalized Variational-Formed Operators. One can generalize the variational formulation to the magnitude operator, Laplacian operator, or higher order Sobolev-space operators in a similar fashion, by computing the inner product of the derivatives of basis functions. Table 1 compares the variational-formed regularizers with traditional regularizers for ZOT, FOT and SOT. Note that the existence of these variational-formed regularizers are guaranteed, because the matrices \mathbf{M} , \mathbf{S} and \mathbf{Q} are by nature symmetric and semi-positive-definite.

Measured by the L_2 -norm over a continuous field, variational-formed regularizers preserve their norms regardless of discretization resolution, because the basis functions ϕ_i already accounts for mesh spacing. In contrast, traditional operators measure the Euclidean norm, thus susceptible to the size of discretization. Norm preservation is a desirable quality that ensures consistent regularization under multi-scale simulations, as will be seen in the Result section.

Imposing Multiple Regularizers. Our proposed variational-formed regularizers are inherently suited for regularization with multiple constraints in the form:

$$\mathbf{u}_H = \operatorname{argmin} \|\mathbf{K}\mathbf{u}_H - \mathbf{u}_T\|_2^2 + \sum_{i=1}^k \lambda_i^2 \|\mathbf{L}_i \mathbf{u}_H\|_2^2 \quad (5)$$

For computational efficiency, one can build a compact constraint (denoted as \mathbf{L}^*) that is equivalent to the superposition of all constraints. \mathbf{L}^* satisfies the condition $\mathbf{L}^{*T} \mathbf{L}_i^* = \sum_{i=1}^k \lambda_i^2 \|\mathbf{L}_i^T \mathbf{L}\|^2$. Each $\mathbf{L}_i^T \mathbf{L}_i$ can be pre-computed using the mesh information only. \mathbf{L}^* can be obtained efficiently without solving each \mathbf{L}_i .

3. Results

Experiment Setup. Our simulation uses a geometric model consisting of a realistic canine heart suspended in a human torso tank created from MRI scans[1]. The tank is filled with a homogeneous electrolytic medium. Both the heart surface and the torso surface are triangulated, and the volume is discretized by a tetrahedral mesh. The heart surface comprises 337 nodes and 670 triangles, the torso surface comprises 771 nodes and 1538 triangles, and the torso volume comprises 27,361 tetrahedra. Epicardial potentials

Table 1. The choice of \mathbf{L} for traditional and variational-formed Tikhonov regularization.

Regularization Type	Traditional Regularizer	Variational Regularizer
ZOT	Identity Matrix	$\mathbf{L}^T \mathbf{L} = \mathbf{M}$
FOT	Hard to Define	$\mathbf{L}^T \mathbf{L} = \mathbf{S}$
SOT	Discrete Laplacian Operator	$\mathbf{L}^T \mathbf{L} = \mathbf{Q}$

Note: \mathbf{L} is associated with the mesh of the heart surface. The matrices \mathbf{M} , \mathbf{S} and \mathbf{Q} are given by $\mathbf{M}_{i,j} = (\phi_i, \phi_j)$, $\mathbf{S}_{i,j} = (\nabla\phi_i, \nabla\phi_j)$, $\mathbf{Q}_{i,j} = (\nabla^2\phi_i, \nabla^2\phi_j)$, $i, j \in \mathcal{H}$. (\cdot) is the inner product. \mathbf{M} is usually named the mass matrix and \mathbf{S} named the stiffness matrix.

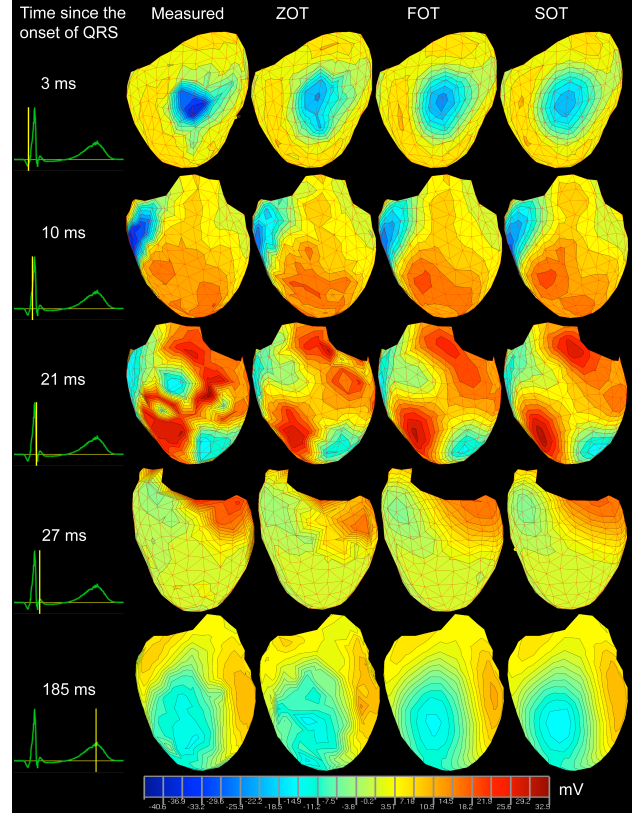


Figure 1. Epicardial potentials calculated under 30dB input white noise. FOT uses the variational-formed gradient operator given by Table 1. For better visualization effect the view is slightly changed at each instant. Color scale: -44.3 mV to 32.9 mV.

are measured *in vivo* via a sock of electrodes surrounding the heart. With the geometry and epicardial potentials, we conduct finite element simulation to obtain the transfer matrix and the torso potentials. After adding noise to the torso potentials, we inversely calculate epicardial potentials using the Tikhonov method. The regularizing parameter λ is determined by the corner of the L-curve, a parametric plotting of $\|\mathbf{L}\mathbf{u}_H\|$ versus the residual error $\|\mathbf{K}\mathbf{u}_H - \mathbf{u}_T\|$. Typically in a L-shape, this curve shows the tradeoff between minimizing the residual error and minimizing the constraint (see Fig 4 for example).

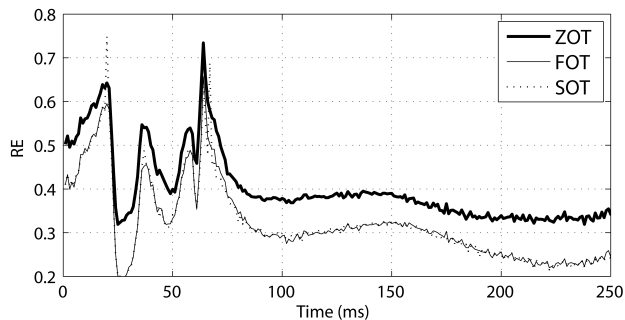


Figure 2. Relative error (RE) of the inverse solutions over a cardiac cycle, corresponding to the test in Fig 1. RE is the ratio of the error to the exact solution, both evaluated by the Euclidean norm. The QRS wave starts at 35ms and ends at 65ms.

Efficacy of the Variational-Formed Gradient Operator as a Regularizer. Fig 1 shows the reconstructed epicardial potentials during a cardiac cycle. The first-order Tikhonov (FOT) uses the variational-formed gradient regularizer, and is compared with the traditional zero-order and second-order Tikhonov methods. FOT consistently yields more accurate solutions than ZOT. Overall FOT and SOT have close performance, but sometimes FOT achieves better potential patterns or iso-potential contours (e.g., the pattern at 10 ms, the saddle point at 21 ms, and the contours at 27 ms). This is reasonable, for FOT aims at capturing gradients whereas SOT aims at curvatures. Fig 2 compares the relative error of the inverse solutions made by the three regularization methods. It confirms that FOT and SOT have close performance while outperforming ZOT.

The Gradient Operator for Ischemia Detection. Transmural ischemia is typically characterized by elevation (implying ischemic regions) and depression (implying border zones) of epicardial potentials during the ST segment. For medium or severe ischemia, a consistent epicardial potential pattern of one maxima between two minima was reported[2]. This pattern can be readily captured by a gradient-constraint-based regularization such as FOT, or the total variation method (TV) which achieves even better estimation of spatial gradients. Rudy *et al.* reported encouraging results by the TV method, using a gradient operator derived from a boundary element formulation[3]. Our variational gradient operator enables the same method when the ECG problem is formulated by finite elements.

Fig 3 shows the reconstruction of epicardial potentials in a medium ischemic condition. Both using the variational-formed gradient operator, the FOT measures the gradient constraint by the L_2 -norm whereas and the TV method by the L_1 -norm. The TV notably outperforms the SOT in reconstructing the gradient field around the elevation region

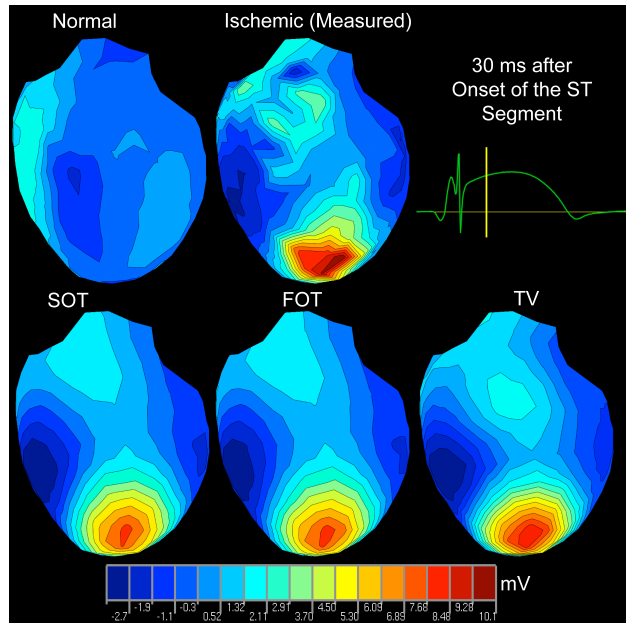


Figure 3. Top row: epicardial potentials (EP) in normal condition compared to the ischemic condition during the ST interval, at an instant marked by the yellow bar in the electrogram. The electrogram reveals the ST elevation typical in ischemia. Bottom row: ischemic epicardial potentials reconstructed by SOT, FOT, and the total variation method (TV), under 30dB input noise. The FOT and TV use the variational-formed gradient operator. Color scale: -3.5 mV to 10.1 mV.

at the apex and in recovering the two minima on both sides of the heart. This means the variational formulation is a promising technique for ischemia detection.

Norm Preservation under Multi-Scale Simulation.

One advantage of the variational-formed operators over traditional discrete operators is that the former preserves the norm under multi-scale simulations. We illustrate this point by comparing the ZOT using the traditional and variational-formed regularizers, as given in Table 1. Fig 4(A) shows the L-curves resulting from the the identity-matrix regularizer. Panel B shows the L-curves using the regularizer derived from the mass matrix. Each regularizer is tested under two resolutions: a coarse Mesh 1 and a uniformly-refined Mesh 2. Mesh 2 yields a discrete inverse problem four times larger than the problem from Mesh 1.

In Panel A, refinement increases both the residual error and the solution norm, shifting the L-curve to the upper right. In Panel B, the L-curve is not much affected by refinement (note the different axis scales in the two panels). The corner of an L-curve typically gives a reasonable regularization. In Panel B, the residual error and the solution norms are preserved at the corner during refinement, whereas in Panel A both terms are nearly doubled by refinement. Note that the size of the inverse solution

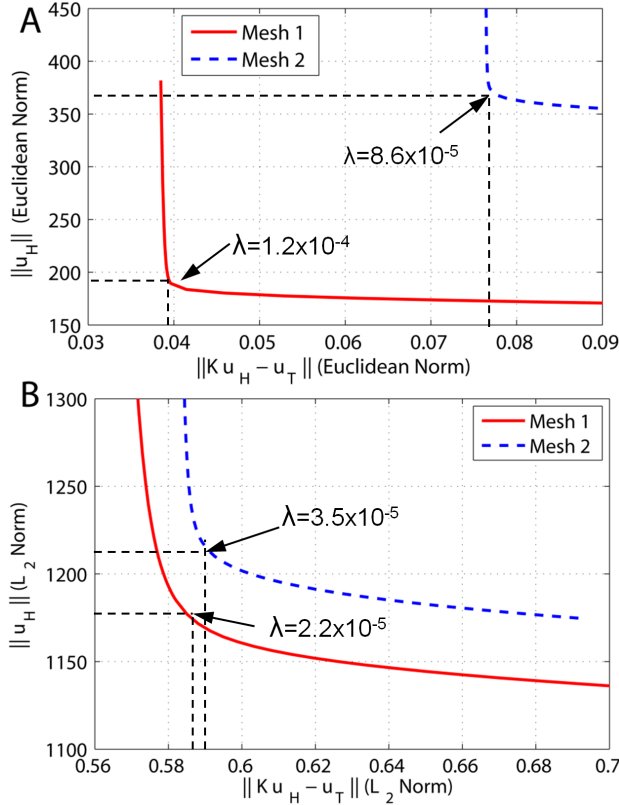


Figure 4. L-curves of the solution norm versus the residual error when ZOT is performed under multi-scale inverse simulations. Mesh 1 has 27,361 tetrahedral elements with 670 triangular elements on the heart surface. Mesh 2 has 60,617 volume elements with 2,680 triangles on the heart surface. Panel A: the regularizer is the identity matrix, and residual error and regularizer are evaluated by the Euclidean norm. Panel B: the regularizer is the Cholesky factor of the mass matrix given by Table 1, evaluated by the continuous L_2 norm. λ gives the value of the regularization parameter at the corner of each L-curve.

vector increases by four times from Mesh 1 to Mesh 2, but the Euclidean norm of the solution vector is only doubled. This means that the traditional ZOT tends to overly smooth the inverse solution under refinement, causing inconsistent regularization under multi-scale simulations.

Fig 5 shows the inverse solutions calculated during the QRS when epicardial potentials exhibit the most diverse distribution. The traditional regularizer yields inconsistent potential patterns over refinement, and the relative error rises from 0.50 to 0.53. In contrast, the variational-formed regularizer maintains the patterns over refinement, and the error drops from 0.48 to 0.42.

4. Discussion and Conclusions

We propose a set of variational-form-based operators for regularizing the inverse ECG problem, especially when

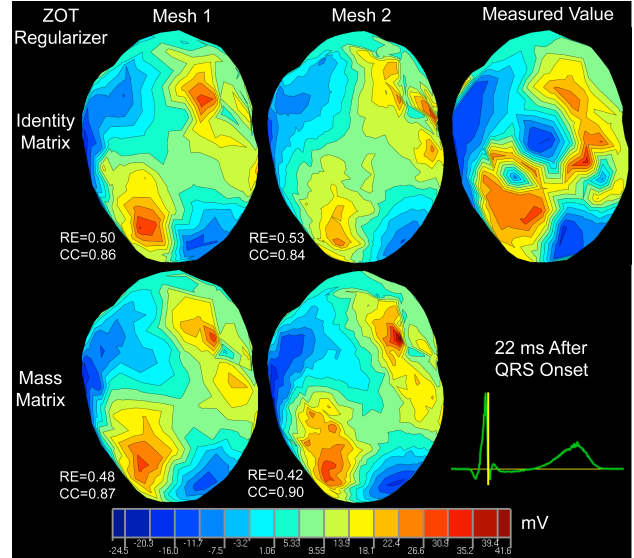


Figure 5. Heart potentials reconstructed under 30dB input noise by ZOT using the traditional and the variational regularizers, corresponding to the L-curves in Fig 4. For each inverse solution, relative error (RE) and correlation coefficient (CC) are given. Color scale: -24.5 mV to 41.6 mV.

the problem is discretized by finite elements. While traditional regularization approaches the inverse problem in a pure linear algebra view, the variational formulation respects the connection between the continuous problem and the discretized problem. This property enables simple construction of the gradient operator, and achieves consistent regularization under multi-scale simulations. We believe the variational formulation may bring insights into other potential-field-based electrocardiographic problems.

References

- [1] MacLeod R, Taccardi B, Lux R. Electrocardiographic mapping in a realistic torso tank preparation. Proc of 17th IEEE Eng in Med and Bio Conf 1995;245–246.
- [2] Hopfenfeld B, Stinstra J, MacLeod R. The effect of conductivity on st-segment epicardial potentials arising from subendocardial ischemia. Annual of Biomed Eng 2005;33(6).
- [3] Ghosh S, Rudy Y. Application of l_1 -norm regularization to epicardial potential solution of the inverse electrocardiography problem. Annals of Biomed Eng 2009;37(5):902–912.

Address for correspondence:

Dafang Wang: dfwang@sci.utah.edu
72 S, Central Campus Dr, WEB Rm 3750
University of Utah, Salt Lake City, 84112, USA